Conductivity of a Disordered Wigner crystal

Ulrich Wulf, Jan Kučera, and E. Sigmund
Technische Universität Cottbus, Fakultät 1, Postfach 101344, 03013 Cottbus, Germany
(Received 19 April 1996)

We extend our previous theory for the ground state of a disordered electron solid to calculate its transport properties. The Coulomb interaction is taken in the Hartree-Fock approximation and the potential of charged impurities in the self-consistent Born approximation. In agreement with recent experiments by Li *et al.* we find, for strong disorder, a linear frequency dependence of the in-phase conductivity. We show how the dc conductivity of the system can be determined in our theory. At strong disorder an algebraic temperature dependence of the conductivity results which is consistent with experiments by Goldman *et al.* [S0031-9007(96)01310-5]

PACS numbers: 72.10.Bg, 71.23.An

In a series of experiments on high-mobility two-dimensional electron gases a metal-insulator transition was found in strong magnetic fields. Depending on the degree of disorder three different mechanisms for the electron localization are possible: First, the formation of an electron crystal which is expected for the clean system when the area $2\pi l^2$ of the "magnetic confinement" of the quantum cyclotron orbits is much smaller than the mean area per electron n^{-1}. Second, the formation of a "glassy" electron solid at intermediate disorder, and third, an Anderson-type single particle localization at dominant disorder. While a few studies have been devoted to the single particle localization [1], the majority of authors interpreted their data in terms of the formation of an electron lattice for filling factors smaller than about $\nu = 1/5$. Arguments are, among others, the thermally activated transport in the linear *I-V* regime [2], the threshold behavior of the electrical transport in the nonlinear regime [3,4], and the detection of the magnetophonon mode in rf experiments [5]. Very little is known about the response properties of the glassy phase which we want to focus on in this Letter. Our previous mean field theory of the ground state of the disordered electron crystal [6] has allowed us to define a glassy phase with a hexagonal short-range order on one hand and a finite density of states at the Fermi level on the other hand. Based on this theory, we develop for the first time a microscopic quantum theory for the transport properties of the disordered electron solid. In the following, we outline our formalism and show that the results of two independent experiments can be understood with the defined glassy phase. First, a recent experiment by Li *et al.* [7] in which a close-to-linear frequency dependence of the real and the imaginary parts of the longitudinal conductivity has been reported. Second, the weak (algebraic) temperature dependence of the longitudinal resistance which turns over to an activated behavior ($\ln R \propto T^{-1}$) in the Wigner crystal regime at very low temperatures as found by Goldman *et al.* [4].

In Fig. 1(a) our approximations for the ground state are shown diagrammatically: The Coulomb interaction is taken in the Hartree-Fock approximation and the disorder potential in the self-consistent Born approximation (SCBA). These approximations are discussed in detail and justified in Ref. [6]. A considerable simplification for the solution of Dyson's equation [Fig. 1(a)] is achieved using a representation $G(\vec{k}, z)$ of the Green's function

$$\begin{aligned} G(\vec{r}, \vec{r}', z) &= \sum_{X,X'} G(X, X', z)\Phi_X(\vec{r})\Phi^*_{X'}(\vec{r}') \\ &= \sum_{\vec{k}X} G(\vec{k}, z)\exp\left(ik_x X - i\frac{k_x k_y l^2}{2}\right) \\ &\quad \times \Phi_X(\vec{r})\Phi^*_{(X-k_y l^2)}(\vec{r}'), \end{aligned} \tag{1}$$

where $G(\vec{k}, z)$ depends on only one wave vector $\vec{k}$ of the hexagonal reciprocal lattice. The $\Phi_X(\vec{r})$ are the lowest Landau-level eigenfunctions in the Landau gauge which depend on the center coordinate X. Since all higher Landau levels are neglected, we can write the exchange term in the same form v_{exc} like the Hartree term v_{dir} [6,8] [see

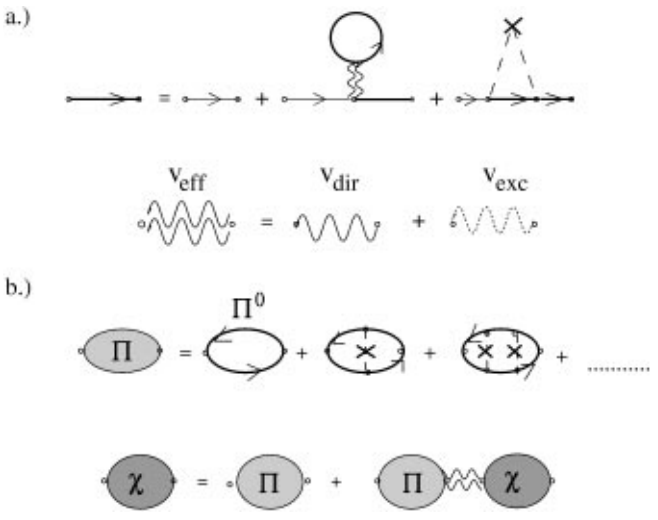

FIG. 1. Our formalism in diagrammatic form: (a) ground state approximation, (b) the response. The upper line in (b) shows the summation of the impurity vertex corrections in the self-consistent Born approximation (dashed lines with crosses), the lower line the inclusion of the Coulomb interaction (double wavy line).

second line of Fig. 1(a)] leading to an effective interaction $v_{\rm eff}$ [Eq. (8)]. As derived in Ref. [9], the density response function $\chi(\vec{r}_1, \vec{r}_2, \omega) = \delta n(\vec{r}_1, \omega)/\delta v_{\rm ext}(\vec{r}_2, \omega)$ to the external potential $v_{\rm ext}(\vec{r}_2, \omega)$ is obtained consistent with our approximation for the Green's function as shown diagrammatically in Fig. 1(b). A similar approximation has been applied in Ref. [10] to a two-dimensional electron gas without lateral modulation. For the description of the electron solid, however, the inclusion of the reciprocal lattice vectors is decisive.

The diagrams in Fig. 1(b) can be evaluated for a system with lateral modulation using a matrix formalism in the space of the reciprocal lattice vectors. In the first step we perform the ladder-sum sum over the SCBA vortex corrections indicated in the upper line of Fig. 1(b). We insert the representation Eq. (1) for the Green's function in the standard expression for the "bare bubble" $\Pi^0(\vec{r}_1, \vec{r}_2, i\omega_n)$ and take the two-dimensional Fourier transform $\Pi^0(\vec{q} + \vec{k}, \vec{q} + \vec{k}', i\omega_n) \equiv \hat{\Pi}^0_{\vec{k},\vec{k}'}(\vec{q}, i\omega_n)$ to find

$$\hat{\Pi}^0_{\vec{k},\vec{k}'}(\vec{q}, i\omega_n) = \frac{\hat{A}_{\vec{k},\vec{k}'}(\vec{q})}{\beta} \sum_{i\omega_n'} \hat{\pi}^0_{\vec{k},\vec{k}'}(\vec{q}, i\omega_n, i\omega_n'), \quad (2)$$

with

$$\hat{\pi}^0_{\vec{k},\vec{k}'}(\vec{q}, i\omega_n, i\omega_n') = \sum_{\vec{k}''} G(\vec{k}'' + \vec{k}, i\omega_n + i\omega_n') G(-\vec{k}'' - \vec{k}', i\omega_n') \times \exp\left[-\frac{il^2}{2} \vec{q} \times (\vec{k} + \vec{k}') \right] \exp\left[\frac{il^2}{2} \vec{k}'' \times (2\vec{q} + \vec{k} + \vec{k}') \right], \quad (3)$$

and

$$\hat{A}_{\vec{k},\vec{k}'}(\vec{q}) = \frac{1}{2\pi l^2} \exp\left[-\frac{(\vec{q} + \vec{k})^2 l^2 + (\vec{q}' + \vec{k}')^2 l^2}{4} \right]. \quad (4)$$

Here $\vec{q}$ is in the first Brillouin zone of the hexagonal reciprocal lattice $\vec{k}$, $\beta = 1/k_B T$, $\omega_n = (2n + 1)\pi/\beta$ is a fermionic Matsubara frequency, and the hat, e.g., in $\hat{\Pi}^0(\vec{q}, \omega_n)$, denotes a matrix in the reciprocal space.

The ladder sum over the vertex corrections of the impurity interaction can now be written as a geometric series

$$\hat{\pi}(\vec{q}, \omega_n, \omega_n') = \hat{\pi}^0(\vec{q}, \omega_n, \omega_n') [\hat{\delta} - \hat{V}^I \hat{\pi}^0(\vec{q}, \omega_n, \omega_n')]^{-1}. \quad (5)$$

The impurity interaction enters through the matrix $\hat{V}^I_{\vec{k},\vec{k}'} = \delta_{\vec{k},\vec{k}'} V_I(\vec{q} + \vec{k})$. For an ensemble of $\delta-$ scatterers with an individual scattering potential $v(r) = V_0 \delta(r)$ we obtain [11]

$$V_I(\vec{q}) = \frac{\Gamma^2}{4} \exp\left[-\frac{\vec{q}^2 l^2}{2} \right], \quad (6)$$

where $\Gamma^2 = 4 n_I V_0^2 / 2\pi l^2$ provides a measure of the impurity strength. $\hat{\Pi}$ is obtained from π by replacing in Eq. (2) $\hat{\Pi}^0$ with $\hat{\Pi}$ and $\hat{\pi}^0$ with $\hat{\pi}$. The Matsubara frequency summation in Eq. (2) can be carried out for each component of the matrix $\hat{\Pi}$ as demonstrated in Ref. [10].

The calculation of the density-density response function χ is now carried out according to the second equation in Fig. 1(b). Using the matrix representation we obtain

$$\hat{\chi}(\vec{q}, \epsilon) = \hat{\Pi}(\vec{q}, \epsilon) [\hat{\delta} - \hat{V}^{\rm eff}(\vec{q}) \hat{\Pi}(\vec{q}, \epsilon)]^{-1}, \quad (7)$$

with $\hat{V}^{\rm eff}_{\vec{k},\vec{k}}(\vec{q}) = \delta_{\vec{k},\vec{k}'} V_{\rm eff}(\vec{q} + \vec{k})$ and

$$V_{\rm eff}(\vec{q}) = \frac{2\pi e^2}{q} \left[1 - \left(\frac{\pi}{2} \right)^{1/2} q l \exp\left(\frac{q^2 l^2}{4} \right) I_0\left(\frac{q^2 l^2}{4} \right) \right]. \quad (8)$$

Here I_0 is the modified Bessel function of the first kind. As shown in Ref. [6] the first factor in Eq. (8) gives the contribution of the Hartree term and the second the Fock term.

The correlation function χ evaluated in Eq. (7) describes the density response to the external potential, $\hat{\chi}_{\vec{k},\vec{k}'}(\vec{q}, \omega) = \delta n(\vec{q} + \vec{k}, \omega)/\delta v_{\rm ext}(\vec{q} + \vec{k}', \omega)$. Through the continuity equation $\omega n(\vec{q}, \omega) = \vec{q} \vec{j}(\vec{q}, \omega)$ we can relate the density response to the induced currents

$$-i\omega \delta n(\vec{q} + \vec{k}, \omega) = (\vec{q} + \vec{k}) \sum_{\vec{k}'} \hat{\sigma}_{\vec{k},\vec{k}'}(\vec{q}, \omega) \times (\vec{q} + \vec{k}') \delta v_{\rm eff}(\vec{q} + \vec{k}', \omega), \quad (9)$$

where $\hat{\sigma}_{\mu,\nu;\vec{k},\vec{k}'}(\vec{q}, \omega) = \delta j_\mu(\vec{q} + \vec{k}, \omega)/\delta E_\nu(\vec{q} + \vec{k}', \omega)$. Assuming a slowly varying external potential $\delta v_{\rm ext}(\vec{r}, t) = \delta v_0 \exp(i\vec{q}\vec{r}) \exp(-i\omega t)$ with $\vec{q} \to 0$ we have to expect short-range components $\delta v_{\rm eff}(\vec{q} + \vec{k}, \omega)$, $\vec{k} \neq 0$ in the effective potential. However, a good approximation is obtained averaging out the short-range components in the effective potential in Eq. (9) ("coarse graining method"). We define

$$\sigma(\vec{q}, \omega) \equiv -\frac{i\omega}{q^2} \frac{\delta n(\vec{q}, \omega)}{\delta v_{\rm eff}(\vec{q} + \omega)} = -\frac{i\omega}{q^2} \frac{\hat{\chi}_{0,0}(\vec{q}, \omega)}{1 + (2\pi e^2/q) \hat{\chi}_{0,0}(\vec{q}, \omega)}. \quad (10)$$

Here $\sigma(\vec{q}, \omega)$ is the longitudinal component $\sigma_{x,x}$ of the conductivity tensor, where the x direction is parallel to $\vec{q}$.

The described formalism is used to evaluate numerically the transport properties of a disordered electron solid at a filling factor $\nu = 1/4$ and a disorder strength of $\Gamma = 0.33e^2/l$. This relatively large filling factor was chosen for numerical convenience, as our previous calculations [6] revealed no qualitative differences between $\nu = 1/4$ and $1/7$. In [6] it was shown that the chosen disorder strength is slightly below a certain critical value. Above this critical value the system remains in the limit $T \to 0$ in a state with crystalline short-range order on one hand but finite density of states at the Fermi level on the other hand. As in the case of an amorphous semiconductor the local order preserves the band structure leading to a tail of the density of states in the forbidden gap of the disorder-free structure. This tail amounts to a more or less sharp local minimum of the density of states around the chemical potential. However, in the present case of weaker disorder this tail vanishes at low temperatures (in our case below $k_BT = 0.005e^2/l$) and we obtain a true energy gap. As we will show transport properties change qualitatively below $k_BT = 0.005e^2/l$ from a phase showing a "metallic" conductivity with a weak (algebraic) temperature dependence to a second phase, where we expect an activated temperature dependence.

In Fig. 2 we consider the frequency dependence of the longitudinal conductivity at four wave vectors which represent the results for a variety of temperatures and wave vectors: For a given $\vec{q}$ we obtain two frequency domains: For small frequencies the transport can be qualitatively understood in a diffusion picture, $\sigma = (dn/d\mu)(-i\omega/q^2)Dq^2/(-i\omega + Dq^2)$ with the diffusion constant D. Then we expect for $\omega < Dq^2$ a parabolic frequency dependence of the real and a negative linear dependence of the imaginary part. At $\omega_0 = Dq^2$ the real part of the conductivity has a turning point and the imaginary part a minimum. This can clearly be seen in the results for the larger wave vectors. For small wave vectors, ω_0 decreases to a very small value where the numerical resolution becomes insufficient. As expected, in the regime of $\omega > Dq^2$ the transport is not diffusive any more and linear frequency dependence $\sigma_1(\vec{q},\omega) = \sigma_1(\vec{q},T) + \sigma_1'(\vec{q}',T)\omega$ of the real part of the conductivity is clearly observed. Another general result is that—as expected—the upper bound of the diffusive frequency regime decreases with vanishing wave vector leaving the regime with linear frequency dependence of σ_1 to start at zero frequency. The imaginary part of the conductivity has a more complex behavior: For frequencies above the diffusive transport regime the imaginary part has one zero and increases slightly less than linearly with further increasing frequency. With decreasing wave vector the conductivity zero shifts to vanishing frequency. For numerical reasons wave numbers with $|\vec{q}| < 0.2|X|$ (see caption Fig. 2) cannot be evaluated so that we have to extrapolate to zero wave vector. In the experiments of Ref. [7], which were performed at finite frequencies, a linear frequency dependence of the real and the imaginary part of the conductivity was found. Deviations were small. This directly agrees with our results for the real part of the conductivity. The sublinear dependence of the imaginary part of the theory can be explained taking into account that the frequency interval probed in the experiments was small on the scale of e^2/l allowing a linear fit to the theory curve.

Since the temperature dependence of the dc conductivity is often probed in experiments we want to demonstrate the extraction of such results in our formalism: Assuming a regular behavior of $\sigma_1(\vec{q},T)$ and $\sigma_1'(\vec{q},T)$ for fixed temperature, we can perform the limit $q \to 0$ as demonstrated in Fig. 3. A good fit of the numerical data is obtained

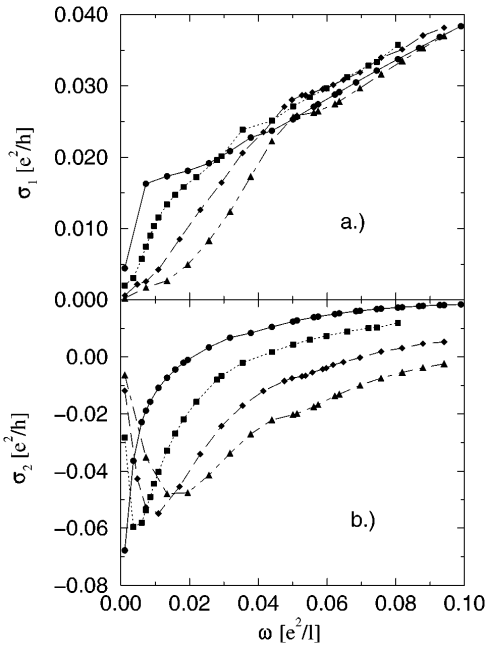

FIG. 2. (a) Real part σ_1 and (b) imaginary part σ_2 of the conductivity vs frequency at $k_BT = 0.01e^2/l$ for $\vec{q} = \alpha\vec{X}$, $\alpha = 0.2$ (circles), 0.4 (squares), 0.6 (diamonds), and 0.8 (triangles). The $\vec{X}$ point at the border of the first Brillouin zone of the hexagonal lattice is defined like in Ref. [12].

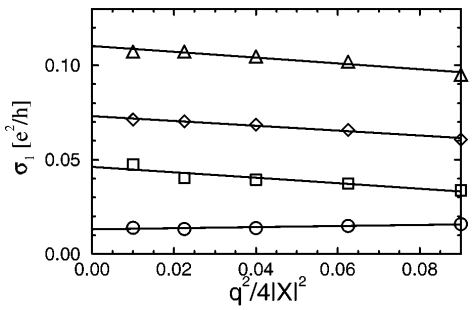

FIG. 3. Extrapolation of $\sigma_1(\vec{q},T)$ (lower part) as defined in the text to zero wave vector at the temperatures $k_BT = 0.01e^2/l$ (circles), $0.02e^2/l$ (squares), $0.03e^2/l$ (diamonds), and $0.04e^2/l$ (triangles), $\vec{q}$ and $\vec{X}$ as defined in Fig. 2. In solid straight lines of a linear regression determining the result for zero wave vector.

assuming $\sigma_1(\vec{q},T) = \sigma_0 + \gamma q^2$ with a free parameter γ. It is found that the procedure for $\sigma_1'(\vec{q},T)$ is analogous.

Figure 4 shows the temperature dependence of σ_0. The arrow marks the temperature below which there is an energy gap comparable to or larger than the thermal energy. Above this temperature we find crystalline short-range order and an enhanced real part of the conductivity showing an algebraic temperature dependence

$$\sigma_0 = s(T - T_0)^r. \tag{11}$$

As can be seen from Fig. 4 the curve for $\sigma_0(T)$ closely follows the increase of the density of states at the chemical potential D_μ, revealing this increase as the origin of the enhanced conductivity. For temperatures below the position of the arrow we expect a turnover to an exponentially activated transport. Because of the small size of the energy gap this range of temperatures is not accessible at the given disorder strength.

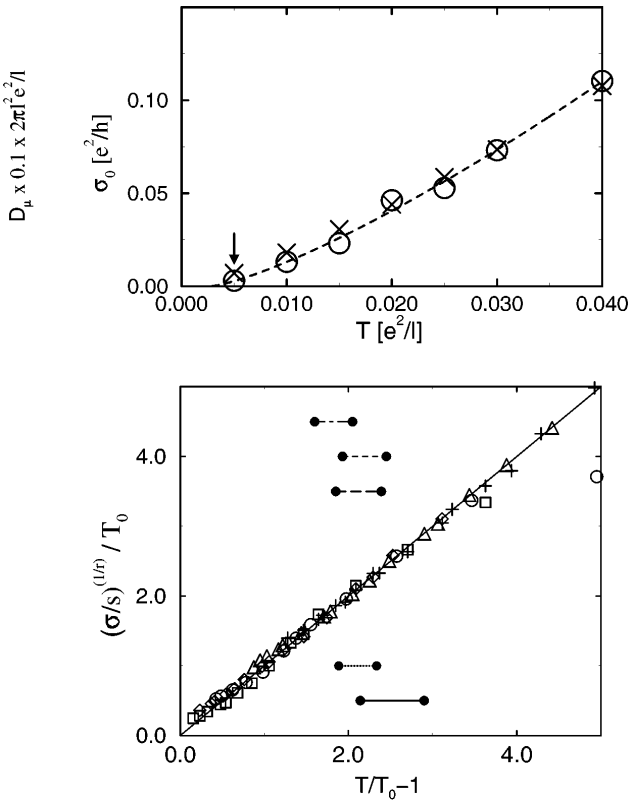

FIG. 4. Upper panel: dc-transport conductivity (in circles, inner label of the y axis) with a fit of an algebraic expression defined in Eq. (11) with the parameters $T_0 = 0.29$, $s = 7.75$ (temperatures in units of $10^{-2}e^2/l$, conductivity in e^2/h), and $r = 1.3$. Marked with crosses the density of states at the chemical potential D_μ (left label of the y axis). Lower panel: Rescaled experimental conductivity $\bar{\sigma}_{\text{exp}} = (\sigma_{\text{exp}}/s)^{1/r}/T_0$ at the filling factors $\nu = 0.215$ [crosses; ($s = 299, r = 1.6, T_0 = 1.35$)], 0.19 [triangles; (825,2.4,2.0)], 0.18 [diamonds; (326,2.1,4.1)], 0.17 [squares; (234,2.0,5.4)], 0.15 [circles; (474,2.7,5.6)], the solid line is the algebraic conductivity in Eq. (11). The experimental temperature intervals for the transition to the crystalline phase at $\nu = 0.215$ (dash-dotted horizontal line), 0.19 (dashed), 0.18 (long-dashed), 0.17 (dotted), and 0.15 (solid).

Experimental results by Goldman *et al.* can be described with Eq. (11). In Ref. [4] these authors found in the regime of electron localization ($R_{xx} > h/\nu e^2$) a turnover from a weak temperature dependence of the longitudinal resistance for larger temperatures to an activated longitudinal resistance ($\ln R \propto T^{-1}$) in the crystal phase. As pointed out in Ref. [13] one can assume in the regime of electron localization a simple matrix relation $\sigma_{xx} = R_{xx}/(R_{xx}^2 + R_{xy}^2)$. Furthermore, the experimental Hall resistance is close to its classical value $R_{xy} = h/\nu e^2$ and can thus be neglected against R_{xx} to yield $\sigma_{xx} = R_{xx}^{-1}$. Under these assumptions we rescale the experimental values $\sigma_{\text{exp}} = 1/R_{xx}$ with filling-factor dependent fit parameters s, T_0, and r as defined in Fig. 4 and find agreement with Eq. (11). The experimental temperatures of the melting transition are found to fall together on the normalized temperature scale at $T/T_0 \approx 3$. In our numerical calculation this is at $T = 8.7 \times 10^{-3}e^2/l$ below which temperature a true gap in the density of states starts to build up, and the Wigner crystal is formed.

In conclusion, we present a microscopic quantum theory of the transport properties of a disordered electron solid. At strong disorder we find a glassy phase. Its transport properties—a close-to-linear frequency dependence and an algebraic temperature dependence of the longitudinal conductivity—are consistent with experimental data by Li *et al.* and Goldman *et al.*

[1] A. A. Shashkin *et al.*, Phys. Rev. Lett. **73**, 3141 (1994); I. V. Kukushkin *et al.*, Phys. Rev. B **53**, R13 260 (1996).
[2] R. L. Willet *et al.*, Phys. Rev. B **38**, 7881 (1988); H. W. Jiang *et al.*, Phys. Rev. Lett. **65**, 633 (1990).
[3] R. L. Willet *et al.*, Phys. Rev. B **40**, 6432 (1989); F. I. B. Williams *et al.*, Phys. Rev. Lett. **66**, 3285 (1991).
[4] V. J. Goldman *et al.*, Phys. Rev. Lett. **65**, 2189 (1990).
[5] E. Y. Andrei *et al.*, Phys. Rev. Lett. **60**, 2765 (1988); M. A. Paalanen *et al.*, Phys. Rev. B **45**, 11 342 (1992).
[6] U. Wulf, Phys. Rev. B **52**, 12 120 (1995).
[7] Y. P. Li *et al.*, Solid State Commun. **95**, 619 (1995).
[8] A. H. MacDonald and S. M. Girvin, Phys. Rev. B **38**, 6295 (1988).
[9] G. Baym and L. P. Kadanoff, Phys. Rev. B **124**, 287 (1961).
[10] D. Antoniou, A. H. MacDonald, and J. C. Swihart, Phys. Rev. B **41**, 5440 (1990).
[11] U. Wulf and A. H. MacDonald, Phys. Rev. B **47**, 6566 (1993).
[12] R. Cote and A. H. MacDonald, Phys. Rev. B **44**, 8759 (1991).
[13] V. J. Goldman, Bo Su, and J. K. Wang, Phys. Rev. B **47**, 10 548 (1993).